

Au/Titania Composite Nanoparticle Arrays with Controlled Size and Spacing by Organic-Inorganic Nanohybridization in Thin Film Block Copolymer Templates

Xue Li,^{*,‡} Jun Fu,[†] Martin Steinhart,[§] Dong Ha Kim,^{*,*†} and Wolfgang Knoll[†]

[†]Max Planck Institute for Polymer Research, Ackermannweg 10, 55128 Mainz, Germany

[‡]School of Chemistry and Chemical Engineering, University of Jinan, Jinan 250022, P. R. China

[§]Max Planck Institute of Microstructure Physics, Weinberg 2, 06120 Halle, Germany

^{*}Division of Nano Sciences and Department of Chemistry, Ewha Womans University, Seoul 120-750, Korea

*E-mail: dhkim@ewha.ac.kr

Received February 22, 2007

A simple approach to prepare arrays of Au/TiO₂ composite nanoparticles by using Au-loaded block copolymers as templates combined with a sol-gel process is described. The organic-inorganic hybrid films with closely packed inorganic nanodomains in organic matrix are produced by spin coating the mixtures of polystyrene-block-poly(ethylene oxide) (PS-*b*-PEO)/HAuCl₄ solution and sol-gel precursor solution. After removal of the organic matrix with deep UV irradiation, arrays of Au/TiO₂ composite nanoparticles with different compositions or particle sizes can be easily produced. Different photoluminescence (PL) emission spectra from an organic-inorganic hybrid film and arrays of Au/TiO₂ composite nanoparticles indicate that TiO₂ and Au components exist as separate state in the initial hybrid film and form composite nanoparticles after the removal of the block copolymer matrix.

Key Words : Au/TiO₂ nanoparticle, Block copolymer, Sol-gel, Organic-inorganic hybrid, Photoluminescence

Introduction

Metal/semiconductor oxide composite nanoparticles are extremely attractive because they exhibit novel optical, electrical, magnetic, and chemical properties that are not found in the individual components.¹⁻³ The possible applications include nanoelectronics device, catalysis, nonlinear optical devices, etc.¹⁻⁵ Titanium dioxide (TiO₂) is one of the most widely studied semiconductor materials due to the wealth of useful applications.^{1,5,6} Recently, TiO₂-based systems containing transition metal ions and noble metals have been investigated extensively to improve the efficiency of the photocatalytic and photoelectrochemical responses.^{1,2}

Several routes to the fabrication of thin films containing nanoparticles of semiconductors and metals have been suggested including physical techniques,^{7,8} chemical methods,^{9,10} or a two-step method consisting of Au(III)-complex chemisorption and subsequent photoreduction.^{2c} Microstructured Au/TiO₂ model catalysts are also produced by combining optical lithography methods for microstructuring with ultrahigh vacuum evaporation for Au nanoparticle deposition.¹¹

In many applications, the ability to use nanoparticle properties for device fabrication will require the formation of highly ordered arrays of nanoparticles.¹² Several approaches have been reported to generate arrays of composite nanoparticles.¹³ However, it is challenging to control the final morphology and composition of the produced nanostructures. There is still a strong demand for simple, facile routes to fabricate arrays of the metal/semiconductor composite nanostructures with different size, spacing or composition.

The self-assembly of diblock copolymers has been recognized as an attractive platform toward highly ordered, periodic

nanoscale structures.¹⁴⁻¹⁷ An increasing number of novel functional nanostructures have been reported from this unique class of polymers,¹⁸⁻²³ for instance, magnetic storage media,²⁴ resists in microelectronics,²⁵ photonic band gap materials,²⁶ planar optical waveguides,²⁷ etc. In particular, it has also been shown that hexagonally ordered 2-dimensional (2D) arrays of metallic, inorganic, semiconductor, and metal/semiconductor nanoparticles could be generated using block copolymer as templates.²⁸⁻³¹

Recently, thin films of amphiphilic poly(styrene-block-ethylene oxide) copolymer (PS-*b*-PEO) with cylindrical PEO microdomains aligned perpendicular to the substrate surface have attracted increasing attention as scaffolds to produce arrays of inorganic nanostructures.^{30,31} Combining sol-gel (SG) process, organic-inorganic hybrid nanostructures can be fabricated with TiO₂ selectively incorporated into the PEO microdomains.³¹ In this work, we extend this methodology to produce arrays of composite Au/TiO₂ composite nanoparticles using Au precursor-loaded block copolymer micelles as templates. Although sol-gel chemistry using block copolymers as structure-directing agent has been extensively exploited to generate highly ordered mesoporous materials,³² no experimental reports have yet been made concerning arrays of metal/semiconductor composite nanoparticles. The present approach involves the fabrication of organic-inorganic hybrid nanocomposite films with TiO₂ and Au precursors incorporated into PEO microdomains. Specifically, we show that the lateral scale of the arrays of composite nanoparticles, *i.e.*, the size of each nanoparticle and spacing, as well as the composition can be finely tuned on the nanometer scale by controlling the relative amount of sol-gel precursor to block copolymer and the loading ratio of HAuCl₄ to EO units in

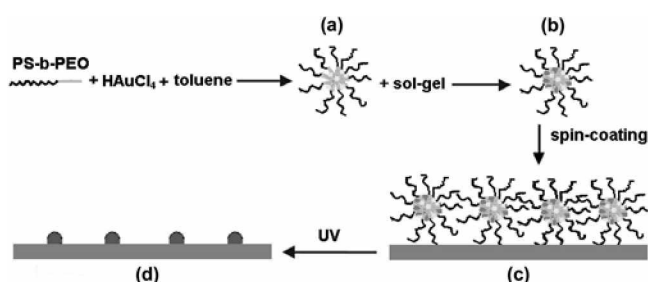


Figure 1. Schematic illustration of the process to produce arrays of Au/TiO₂ composite nanoparticles. (a) Formation of Au-loaded micellar solution of PS-*b*-PEO block copolymers in toluene. (b) The Au-loaded micellar solution is mixed with the desired amount of sol-gel precursor solution; titania precursor incorporates into the PEO/HAuCl₄ domains. (c) Preparation of an organic-inorganic hybrid film by spin coating the mixed solution on a silicon substrate. (d) Arrays of pure Au/TiO₂ composite nanoparticles obtained after removal of the block copolymer template.

the block copolymer. The overall procedure for the generation of Au/TiO₂ composite nanoparticles arrays is schematically illustrated in Figure 1.

Experimental Part

Materials. Asymmetric poly(styrene-block-ethylene oxide) block copolymer (PS-*b*-PEO) with a polydispersity index of 1.05 was purchased from Polymer Source, Inc. The number average molecular weights of PS and PEO blocks are 19000 g/mol and 6400 g/mol, respectively. Titanium tetra-isopropoxide (TTIP, 97%), and tetrachloroauric (III) acid (HAuCl₄·xH₂O, M_w = 333.79) were purchased from Aldrich and used as received. Analytical grade toluene, isopropanol and hydrochloric acid (HCl, 37%) were purchased from Laborbedarf GmbH.

Substrates. Silicon (Si) wafers with a native oxide layer (ca. 2.5 cm × 2.5 cm) were cleaned in a piranha solution (70/30 v/v of concentrated H₂SO₄/30% H₂O₂, **Caution!** Piranha solution reacts violently with organic compounds and should not be stored in closed containers.) at 80 °C for 30 min, thoroughly rinsed with Milli-Q water, and then blown dry with nitrogen gas.

Film Preparation. A 1.0 wt% toluene solution of the PS-*b*-PEO diblock copolymer containing an equivalent amount of HAuCl₄ precursor was stirred for at least 12 h to make a clear solution. The molar ratio of HAuCl₄/EO was adjusted to 0.1. Sol-gel (SG) precursor solutions were prepared as described previously.³¹ The desired amount of sol-gel precursor solution was added into Au-loaded PS-*b*-PEO solution and stirred for 30 min to make the initial common solution, denoted PS-*b*-PEO/HAuCl₄/SG. The amount of precursors relative to the block copolymers (ϕ) was adjusted from 7.0 to 20.0 v/v%.

The hybrid inorganic-organic films were produced simply by spin coating the common solution on a piece of Si substrate at 2500 rpm. To adjust the film thickness, the initial mixed solution was diluted with toluene. The obtained films were dried under ambient condition to induce crosslinking

of the sol-gel precursor. The film thickness was about 48 nm as measured by a surface profiler (Tencor-10).

In order to remove the block copolymer template and reduce HAuCl₄ into metallic Au, the films were treated with deep UV irradiation in air ($\lambda = 254$ nm, 30W) for 2 days.³³

Characterization. AFM height and phase contrast images were obtained using a Digital Instruments Dimension 3100 scanning force microscope in the tapping mode with Olympus cantilever with spring constants ranging between 33.2 and 65.7 N/m and a resonant frequency of 277.3-346.3 Hz (as specified by the manufacturer). Field emission scanning electron microscopy (FESEM) images were obtained with a LEO 1530 "Gemini". The average diameters of the inorganic domains containing titania and gold were determined Image J program (NIH). The center-to-center distance between domains were calculated from AFM images using Nanoscope software (Nanoscope III 5.12r3). XPS measurements were performed on a Perkin-Elmer-Physical Electronics 5100 with Mg K α excitation (400 W). Spectra were obtained at a take-off angle of 15°. Photoluminescence (PL) spectra were measured using a SPEX FLUOROLOG II (212) instrument at an excitation wavelength of 350 nm and 260 nm. The hybrid films were treated at 90 °C for 1 h in vacuum or with UV light for 2 days in air before PL measurement.

Results and Discussion

The AFM height images of the hybrid films spin-coated from the initial PS-*b*-PEO/HAuCl₄/SG mixed solutions with different amount of SG precursor are shown in Figure 2. The

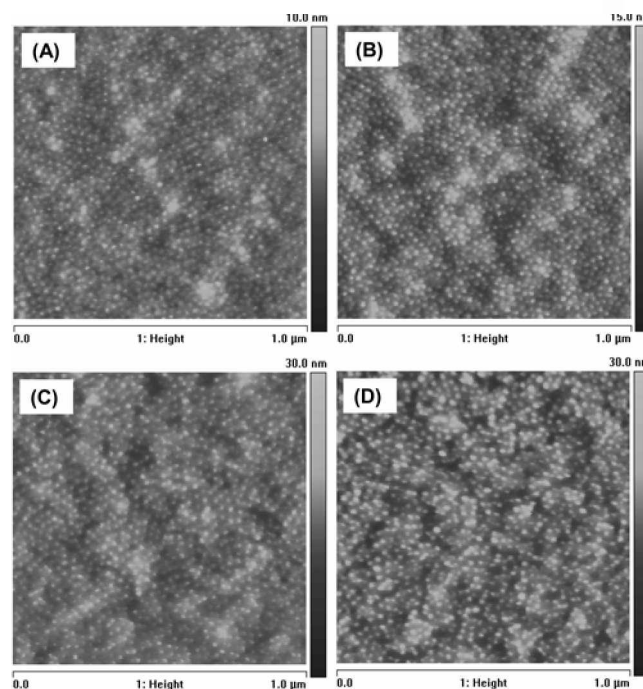


Figure 2. AFM height contrast images of the surfaces of the spin-coated PS-*b*-PEO/HAuCl₄/SG films with different amount of sol-gel precursors: (a) 7.0%; (b) 10.0%; (c) 15.0%; (d) 20.0%. The film thickness is about 48 nm. The images show 1 μ m × 1 μ m area on the surface.

brighter regions in the phase images correspond to the inorganic domains.^{21,31} Highly dense arrays of inorganic nanoparticles in organic matrix were observed when ϕ increases from 7.0% to 20.0%, which is similar to the results obtained in the Au-free PS-*b*-PEO/SG system.³¹ One can see from Figure 2 that the hybrid film with a SG precursor amount of $\phi \sim 10\%$ exhibits well ordered, hexagonal packing with a relatively uniform particle size. Such an optimum SG content in terms of the long-range order was also observed in our previous work.³¹ The surface morphologies of the hybrid films were independent of the film thickness in the range of 10–50 nm explored in this study.

Compared to the previous PS-*b*-PEO/SG system,³¹ the addition of HAuCl₄ has a noticeable influence on the trend of the lateral dimension of the inorganic domains at the surface of a hybrid PS-*b*-PEO/HAuCl₄/SG film with increasing ϕ . Figure 3 shows the SEM images of about 12 nm thick PS-*b*-PEO/HAuCl₄/SG films with different amounts of SG precursors on Si substrates. The average domain size (D) and the center-to-center distance (d_{c-c}) are displayed in Figure 3e. The D values are about 10.5 ± 3.5 , 13.4 ± 2.4 , 15.1 ± 3.2 , and 15.6 ± 3.6 nm and the d_{c-c} values are about 25.0, 25.6, 26.4, and 27.8 nm, for samples with ϕ values of 7.0, 10.0, 15.0, and 20%, respectively. Both D and d_{c-c} increase monotonically with increasing ϕ , which are different from the results observed in the PS-*b*-PEO/SG system.³¹ This result may be explained as follows: PS-*b*-PEO can form micelles in a non-polar solvent (such as toluene used in this study). With the addition of Au precursor HAuCl₄, it forms a complex with the EO units.^{28c} Titania SG precursor is composed of TTIP, HCl (37%), toluene and isopropanol. When the SG precursor is added into the PS-*b*-PEO/HAuCl₄ solution, isopropanol and small amounts of water are easily absorbed into the micellar cores due to the existence of

HAuCl₄ in the PEO domains. Since this effect would cause the aggregation number of the block copolymer micelles to increase,³⁴ it is reasonable to deduce that the micelle size increases with increasing ϕ . On the other hand, the Au precursors uniformly distribute inside PEO domains to form composites with the SG precursors that help to prevent the SG precursors from self-aggregation. This effect may preclude the macro-phase separation of SG precursors from the BCP domains. Therefore, the domain size of the TiO₂ nanoparticles increases with increasing ϕ after SG incorporates into the PEO domains selectively due to strong interaction between the SG precursor and the PEO domains containing HAuCl₄ precursor. With the assumption that the SG precursor is uniformly distributed in the micelles domains,³¹ the center-to-center distance (d_{c-c}) will also increase due to the increase of the micelle size with increasing ϕ . When the SG content is less than $\phi \sim 20\%$, the PEO domains could include all the SG precursor molecules, while macrophase separation occurred with a further increase of ϕ to 30%.

The chemical identity of the surface of a spin-coated PS-*b*-PEO/HAuCl₄/SG10 film was investigated by XPS analysis. The survey spectrum clearly reveals that Ti, O, C, and Au elements exist in the hybrid film, as shown in Figure 4a. Figure 4b is the high resolution Ti_{2p} spectrum and the characteristic peaks of Ti_{2p_{3/2}} and Ti_{2p_{1/2}} in TiO₂ were observed at 459.4 eV and 465.2, respectively.³⁵ The peaks at 457.6 eV and 455.3 eV due to other titania species such as Ti_{2p_{3/2}} in Ti₂O₃ or TiO were not observed.³⁶ Therefore, it is concluded from the XPS results that the titania nanoparticles in the hybrid film are mainly composed of TiO₂.

In order to generate arrays of pure Au/TiO₂ composite nanoparticles on the silicon substrate from the initial hybrid organic-inorganic films, the block copolymer templates were removed by deep UV irradiation. HAuCl₄ is reduced simul-

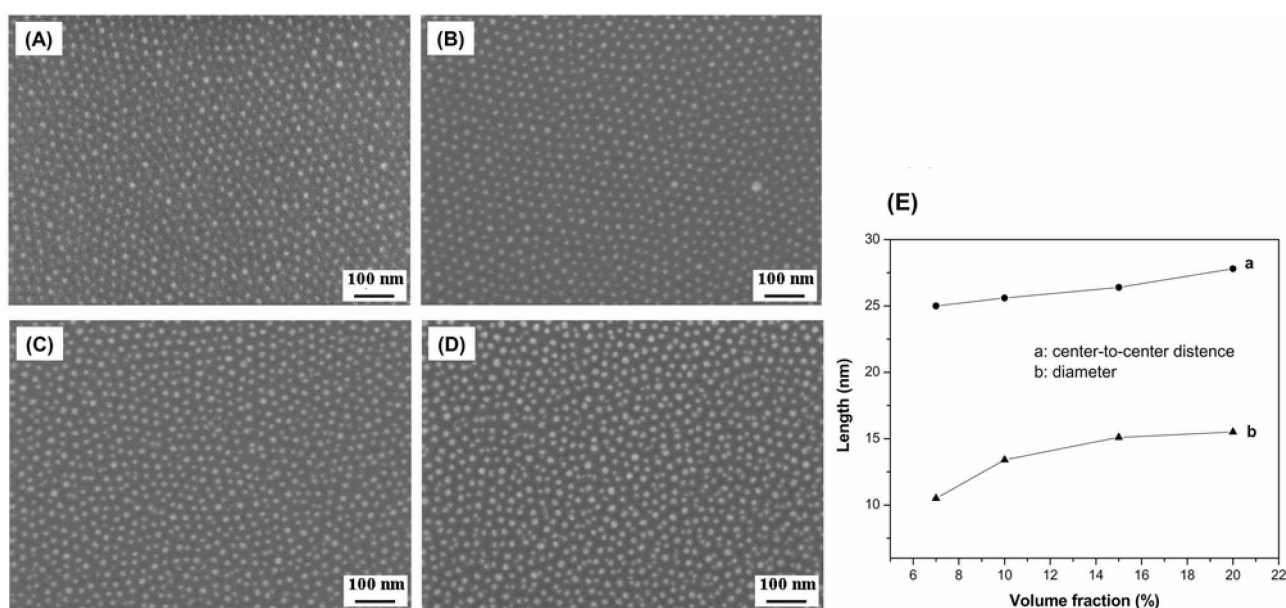


Figure 3. FESEM images of the spin-coated PS-*b*-PEO/HAuCl₄/SG films with different amount of sol-gel precursors: (a) 7.0%; (b) 10.0%; (c) 15.0%; (d) 20.0%. The film thickness is about 12 nm. (e) The average diameter of the inorganic domains, D , and the center-to-center distance between them, d_{c-c} , as a function of the amount of sol-gel precursors. The scale bar at lower left of each SEM image represents 100 nm.

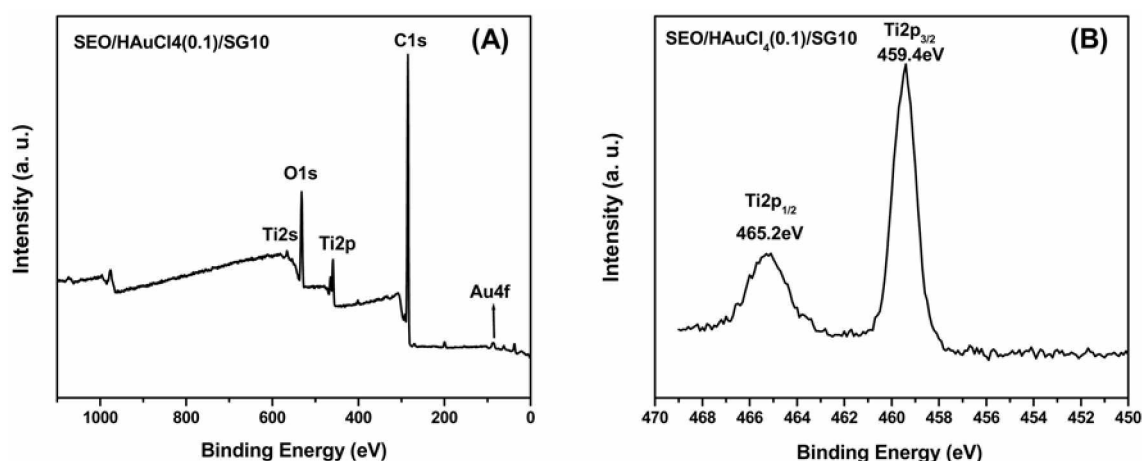


Figure 4. XPS survey (a) and high-resolution XPS Ti_{2p} spectra (b) of the surface of a spin-coated PS-*b*-PEO/HAuCl₄/SG10 film.

taneously into metallic Au during this irradiation process.^{33,37} It should be noted that arrays of composite nanoparticles could be obtained only from hybrid micellar films of PS-*b*-PEO/HAuCl₄/SG of the order of one monolayer thickness because the inorganic domains in thicker films (*e.g.* 48 nm), which do not form cylinders perpendicular to the substrate surface, collapse to form irregular arrays after matrix removal. Figure 5 shows the SEM image of arrays of Au/TiO₂ composite nanoparticles obtained from the hybrid films of about 12 nm thickness obtained by UV exposure in air for 2 days. The average particle size is measured to be 15.7 ± 3.5 nm, 18.1 ± 2.8 nm, 20.9 ± 2.8 nm, and 20.2 ± 4.5 nm for samples with ϕ values of 7.0, 10.0, 15.0, and 20%, respectively. XPS measurement was also performed to determine the chemical composition of the resulting composite nanoparticles. The spectrum of Ti_{2p} from the film after

removal of the block copolymer is similar to that from the hybrid film (Figure 3b). Characteristic peaks of Au⁰ were observed at binding energies of 87.5 eV (Au4f_{5/2}) and 84.0 eV (Au4f_{7/2}).³⁵ Therefore, it is concluded that these nanoparticles contain metallic Au. More in-depth analysis of the individual nanoparticle is in progress by high-resolution transmission electron microscopy.

We explore the photoluminescence (PL) properties of the hybrid PS-*b*-PEO/HAuCl₄/SG films and arrays of Au/TiO₂ composite nanoparticles with an excitation wavelength of 350 nm and 260 nm, respectively. Figure 6 shows the representative PL spectra from a spin-coated film and arrays of Au/TiO₂ nanoparticles with ϕ value of 10.0%. It can be seen from Figure 6a and b, that the initial hybrid samples exhibit the broadband PL with main peak located at about 420 nm under photoexcitation at 350 nm, which can be attributed to

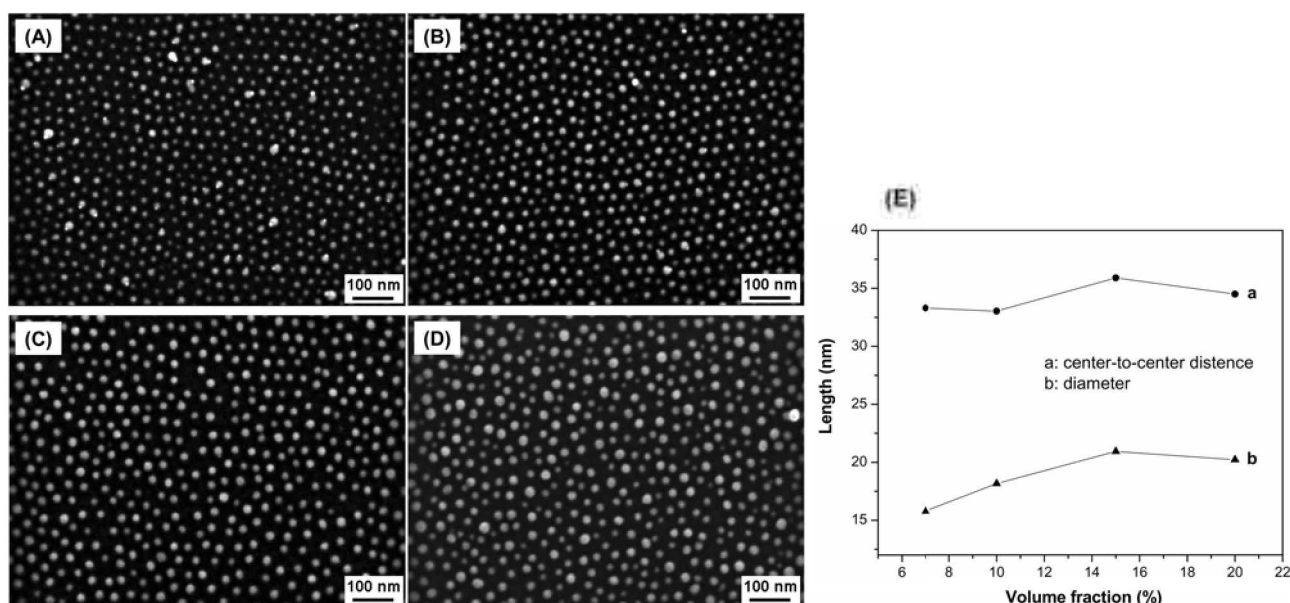


Figure 5. FESEM images of arrays of Au/TiO₂ nanoparticles obtained from the hybrid PS-*b*-PEO/HAuCl₄/SG films after removal of the block copolymer matrix by exposing the samples to UV light for 2 days in air: (a) 7.0%; (b) 10.0%; (c) 15.0%; (d) 20.0%. (e) The average diameter of Au/TiO₂ nanoparticles, D , and the center-to-center distance between them, d_{c-c} , as a function of the amount of sol-gel precursors. The scale bar at lower left of each SEM image represents 100 nm.

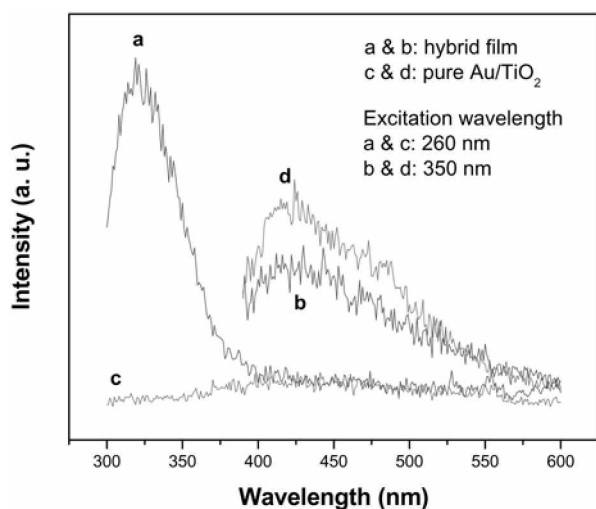


Figure 6. (a) and (b): PL spectra of the hybrid PS-*b*-PEO/HAuCl₄/SG10 film. (c) and (d): PL spectrum from arrays of Au/TiO₂ composite nanoparticles obtained after removal of the PS-*b*-PEO template by deep UV irradiation. The excitation wavelength used in (a)-(c) is 260 nm and 350 nm in (b) and (d), respectively.

the PL spectra of TiO₂ nanoparticles.^{38a} The physical origin of the fluorescence may be interpreted in terms of the emission from the radiative recombination of self-trapped excitons localized within TiO₆ octahedra and oxygen vacancies.³⁸ It is worthwhile to note that the Au nanoparticles in the spin-coated hybrid film exhibit a PL at about 320 nm with a photoexcitation wavelength at 260 nm, which may be assigned to radiative recombination of Fermi level electrons and *sp*- or *d*-band holes.³⁹ After removal of the block copolymer matrix, the PL spectrum of the arrays of Au/TiO₂ composite nanoparticles exhibits only a broadband with a main peak centered at about 420 nm and 455 nm with photoexcitation at 260 nm and 350 nm, respectively. This may be attributed to the structural changes of the Au and TiO₂ nanoparticles. It can be deduced from Figure 6 that the Au and TiO₂ nanoparticles exist in separate domains each other in the hybrid films based on the observation that the PL emission from both the TiO₂ and Au nanoparticles in the hybrid film can be observed. However, the Au and TiO₂ will contact each other if the block copolymer template is removed. Under excitation, the Au nanoparticles are photoexcited due to plasmon resonance, and charge separation occurs by the transfer of photoexcited electrons from the Au particle to the TiO₂ conduction band.⁴⁰ Therefore, PL peak of Au nanoparticles does not appear independently from Au/TiO₂ composite nanoparticles under excitation wavelength of 260 nm. In comparison with TiO₂ nanoparticles, no noticeable difference was found from Au/TiO₂ composite nanoparticles, which is consistent with the previous results.^{29,41}

Conclusions

We presented a simple route to produce arrays of Au/TiO₂ composite nanoparticles using Au-loaded micelles of PS-*b*-PEO block copolymers as templates combining with sol-gel

process. Sol-gel precursors could be selectively incorporated into the PEO/HAuCl₄ domains in the Au-loaded PS-*b*-PEO solution. After spin coating, organic/inorganic hybrid films with dense arrays of inorganic domains containing TiO₂ and Au embedded in an organic matrix were generated. The size of each nanoparticle and the characteristic spacing of the arrays could be controlled by varying the relative amounts of the SG precursors versus block copolymers. By removing the organic template with deep UV irradiation, arrays of pure Au/TiO₂ composite nanoparticles could be obtained with controlled lateral scale on a substrate surface. The initial organic/inorganic hybrid film and the Au/TiO₂ composite nanoparticles array exhibit different fluorescence emissions spectra, indicating that the TiO₂ and Au keep their respective domains in the as-cast, initial films. This work demonstrates a simple, low-cost method with potential applications in photocatalysis, as energy conversion sensors, or as a model system to study the mechanism of photochemistry in nanopatterned media.

Acknowledgements. Dr. X. Li acknowledges the supports of the National Natural Science Foundation of China (20674030), Shandong Natural Science Foundation (Y2006B02) and the Doctorial Foundation of University of Jinan (B0541). This work was supported by the Seoul Research and Business Development Program (10816) and the Korea Research Foundation Grant funded by the Korean Government (MOEHRD, Basic Research Promotion Fund) (KRF-2006-003-D00138). The authors are indebted to Jian Wei Chai at the Institute of Materials Research Engineering (IMRE) in Singapore for the XPS analysis, Gunnar Glasser and Hansjörg Menges at the Max Planck Institute for Polymer Research for the SEM and PL measurements, respectively.

References

- (a) Linsebigler, A.; Lu, G.; Yates, J. T. *Chem. Rev.* **1995**, *95*, 735-758. (b) Jakob, M.; Levanon, H.; Kamat, P. V. *Nano Lett.* **2003**, *3*, 353-358. (c) Naoi, K.; Ohko, Y.; Tatsuma, T. *J. Am. Chem. Soc.* **2004**, *126*, 3664-3668. (d) Cozzoli, P. D.; Comparelli, R.; Fanizza, E.; Currì, M. L.; Agostiano, A.; Laub, D. *J. Am. Chem. Soc.* **2004**, *126*, 3868-3879.
- (a) Rolison, D. R. *Science* **2003**, *299*, 1698-1701. (b) Sun, B.; Vorontsov, A. V.; Smirniotis, P. G. *Langmuir* **2003**, *19*, 3151-3156. (d) Soejima, T.; Tada, H.; Kawahara, T.; Ito, S. *Langmuir* **2002**, *18*, 4191-4194.
- (a) Willner, I.; Patolsky, F.; Wasserman, J. *Angew. Chem. Int. Ed.* **2001**, *40*, 1861-1864. (b) Cao, Y.; Banin, U. *Angew. Chem. Int. Ed.* **1999**, *38*, 3692-3694. (c) Wang, Z.; Chumanov, G. *Adv. Mater.* **2003**, *15*, 1285-1289. (d) Yu, S.; Yoshimura, M. *Adv. Funct. Mater.* **2002**, *12*, 9-15.
- (a) Schneider, J. J. *Adv. Mater.* **2001**, *13*, 529-533.
- (a) Moser, W. R. *Advanced Catalysis and Nanostructured Materials*, Academic Press: San Diego, CA, 1990. (b) Schiavello, M. *Photocatalysis and Environment, Trends and Applications*, Kluwer Press: The Netherlands, 1988. (c) Pelizzetti, E.; Serpone, N. *Photocatalysis: Fundamentals and Applications*, Wiley: New York, 1989.
- (a) Oregan, B.; Gratzel, M. *Nature* **1991**, *353*, 737-740. (b) Diebold, U. *Surf. Sci. Rep.* **2003**, *48*, 53-229. (c) Matthews, R. W. *J. Catal.* **1988**, *111*, 264-272.

7. Arnold, G. W. *J. Appl. Phys.* **1975**, *46*, 4466-4473.
8. Tanahashi, I.; Manabe, Y.; Tohda, T.; Sasaki, S.; Nakamura, A. *J. Appl. Phys.* **1996**, *79*, 1244-1249.
9. (a) He, J.; Ichinose, I.; Fujikawa, S.; Kunitake, T.; Nakao, A. *Chem. Mater.* **2002**, *14*, 3493-3500. (b) He, J.; Ichinose, I.; Kunitake, T.; Nakao, A. *Langmuir* **2002**, *18*, 10005-10010.
10. (a) Pastoriza-Santos, I.; Koktysh, D. S.; Mamedov, A. A.; Giersig, M.; Kotov, N. A.; Liz Marzan, L. M. *Langmuir* **2000**, *16*, 2731-2735. (b) Tom, R. T.; Nair, A. S.; Singh, N.; Aslam, M.; Nagendra, C. L.; Philip, R.; Vijayamohan, K.; Pradeep, T. *Langmuir* **2003**, *19*, 3439-3445.
11. Kielbassa, S.; Kimme, M.; Behm, R. J. *Langmuir* **2004**, *20*, 6644-6650.
12. (a) Schenhar, R.; Norsten, T. B.; Rotello, V. M. *Adv. Mater.* **2005**, *17*, 657-669. (b) Bookstaller, M. R.; Kolb, R.; Thomas, E. L. *Adv. Mater.* **2001**, *13*, 1783-1786.
13. (a) Bullen, H. A.; Garrett, S. J. *Nano Lett.* **2002**, *2*, 739-745. (b) Moritz, T.; Reiss, J.; Diesner, K.; Su, D.; Chemseddine, A. *J. Phys. Chem. B* **1997**, *101*, 8052-8053. (c) Burnside, S. D.; Shklover, V.; Barbe, C.; Comte, P.; Arendse, F.; Brooks, K.; Grätzel, M. *Chem. Mater.* **1998**, *10*, 2419-2425.
14. Hamley, I. W. *The Physics of Block Copolymers*; Oxford University Press: New York, 1998.
15. Fredrickson, G. H.; Bates, F. S. *Annu. Rev. Mater. Sci.* **1996**, *26*, 501-550.
16. Fasolka, M. J.; Mayes, A. M. *Annu. Rev. Mater. Res.* **2001**, *31*, 323-355.
17. Hashimoto, T.; Shibayma, M.; Fujimura, M.; Kawai, H. *Block Copolymers. Science and Technology*; Meier, D. J., Ed.; Harwood Academic: London, 1983; pp 63-108.
18. Lazzari, M.; López-Quintela, M. A. *Adv. Mater.* **2003**, *15*, 1583-1594.
19. (a) Hamley, I. W. *Angew. Chem. Int. Ed.* **2003**, *42*, 1692-1712. (b) Hamley, I. W. *Nanotechnology* **2003**, *14*, R39-R54.
20. Soler-Illia, G. J. de A. A.; Crepaldi, E. L.; Grosso, D.; Sanchez, C. *Curr. Opin. Coll. Inter. Sci.* **2003**, *8*, 109-126.
21. (a) Förster, S.; Plantenberg, T. *Angew. Chem. Int. Ed.* **2002**, *41*, 688-714. (b) Förster, S.; Konrad, M. *J. Mater. Chem.* **2003**, *13*, 2671-2688. (c) Förster, S.; Antonietti, M. *Adv. Mater.* **1998**, *10*, 195-217. (d) Kleitz, F.; Kim, T.-W.; Ryoo, R. *Bull. Kor. Chem. Soc.* **2005**, *26*, 1653-1668. (e) Bae, J. Y.; Choi, S.-H.; Bae, B. S., *Bull. Kor. Chem. Soc.* **2006**, *27*, 1562-1566.
22. Park, C.; Yoon, J.; Thomas, E. L. *Polymer* **2003**, *44*, 6725-6760.
23. Segalman, R. E. *Mater. Sci. Eng. R* **2005**, *48*, 191-226.
24. Thurn-Albrecht, T.; Schotter, J.; Kästle, G. A.; Emley, N.; Shibauchi, T.; Krusin-Elbaum, L.; Guarini, K.; Black, C. T.; Tuominen, M. T.; Russell, T. P. *Science* **2000**, *290*, 2126-2129.
25. Park, M.; Harrison, C.; Chaikin, P. M.; Register, R. A.; Adamson, D. H. *Science* **1997**, *276*, 1401-1404.
26. Urbas, A. M.; Maldovan, M.; DeRege, P.; Thomas, E. L. *Adv. Mater.* **2002**, *14*, 1850-1853.
27. Kim, D. H.; Lau, K. H. A.; Robertson, J. W. F.; Lee, O. J.; Jeong, U.; Lee, J. I.; Hawker, C. J.; Russell, T. P.; Kim, J. K.; Knoll, W. *Adv. Mater.* **2005**, *17*, 2442-2446.
28. (a) Kästle, G.; Boyen, H.-G.; Weigl, F.; Lengli, G.; Herzog, T.; Ziemann, P.; Riethmüller, S.; Mayer, O.; Hartmann, C.; Spatz, J. P.; Möller, M.; Ozawa, M.; Banhart, F.; Garnier, M. G.; Oelhafen, P. *Adv. Funct. Mat.* **2003**, *13*, 853-861. (b) Spatz, J. P.; Mösser, S.; Hartmann, C.; Möller, M.; Herzog, T.; Krieger, M.; Boyen, H.-G.; Ziemann, P. *Langmuir* **2000**, *16*, 407-415. (c) Spatz, J. P.; Roescher, A.; Möller, M. *Adv. Mater.* **1996**, *8*, 337-340.
29. (a) Li, X.; Lau, K. H. A.; Kim, D. H.; Knoll, W. *Langmuir* **2005**, *21*, 5212-5217. (b) Li, X.; Göring, P.; Pippel, E.; Steinhart, M.; Kim, D. H.; Knoll, W. *Macromol. Rapid Commun.* **2005**, *26*, 1173-1178.
30. (a) Kim, D. H.; Jia, X.; Lin, Z.; Guarini, K. W.; Russell, T. P. *Adv. Mater.* **2004**, *16*, 702-706. (b) Kim, D. H.; Kim, S. H.; Lavery, K.; Russell, T. P. *Nano Letters* **2004**, *4*, 1841-1844.
31. (a) Kim, D. H.; Sun, Z. C.; Russell, T. P.; Knoll, W.; Gutmann, J. S. *Adv. Funct. Mater.* **2005**, *15*, 1-6. (b) Sun, Z.; Kim, D. H.; Wolkenhauer, M.; Bumbui, G. G.; Knoll, W.; Gutmann, J. S. *ChemPhysChem* **2006**, *7*, 370-378.
32. (a) Yang, P. D.; Deng, T.; Zhao, D. Y.; Feng, P. Y.; Pine, D.; Chmelka, B. F.; Whitesides, G. M.; Stucky, G. D. *Science* **1998**, *282*, 2244-2246. (b) Yang, P. D.; Zhao, D. Y.; Margolese, D. I.; Chmelka, B. F.; Stucky, G. D. *Nature* **1998**, *396*, 152-155. (c) Brinker, C. J.; Lu, Y.; Sellinger, A.; Fan, H. *Adv. Mater.* **1999**, *11*, 579-585. (d) Soler-Illia, G. J. de A. A.; Sanchez, C.; Lebeau, B.; Patarin, J. *Chem. Rev.* **2002**, *102*, 4093-4138. (e) Göltner, C. G.; Henke, S.; Weissenberger, M. C.; Antonietti, M. *Angew. Chem. Int. Ed.* **1998**, *37*, 613-616.
33. Haseloh, S.; Choi, S. Y.; Mamak, M.; Coombs, N.; Petrov, S.; Chopra, N.; Ozin, G. A. *Chem. Commun.* **2004**, *13*, 1460-1461.
34. Vagberg, L. J. M.; Cogan, K. A.; Gasto, A. P. *Macromolecules* **1991**, *24*, 1670-1677.
35. (a) McKay, J. M.; Henrich, V. E. *Surf. Sci.* **1984**, *137*, 463-472. (b) Zimmermann, R.; Steiner, P.; Claessen, R.; Reinert, F.; Hüfner, S. *J. Electron Spec. Relat. Phenom.* **1998**, *96*, 179-186.
36. (a) Brust, M.; Walker, M. *J. Chem. Soc., Chem. Commun.* **1994**, 801-802. (b) Boyen, H. G.; Kästle, G. *Science* **2002**, *297*, 1533-1536. (c) Juodkazis, K.; Juodkazyte, J.; Jasulaitiene, V.; Lukinskas, A.; Sebek, B. *Electrochem. Commun.* **2000**, *2*, 503-507.
37. Ouyang, M.; Yuan, C.; Muisener, R. J.; Boulares, A.; Koberstein, J. T. *Chem. Mater.* **2000**, *12*, 1591-1596.
38. (a) Zhang, W. F.; Zhang, M. S.; Yin, Z.; Chen, Q. *Appl. Phys. B* **2000**, *70*, 261-265. (b) Tang, H.; Berger, H.; Schmid, P. E.; Lévy, F.; Burri, G. *Solid State Commun.* **1993**, *87*, 847-850. (c) Lei, Y.; Zhang, L. D.; Meng, G. W.; Li, G. H.; Zhang, X. Y.; Liang, C. H.; Chen, W.; Wang, S. X. *Appl. Phys. Lett.* **2001**, *78*, 1125-1127.
39. Wilcoxon, J. P.; Martin, J. E.; Parsapour, F.; Wiedenman, B.; Kelley, D. F. *J. Chem. Phys.* **1998**, *108*, 9137-9143.
40. Tian, Y.; Tatsuma, T. *J. Am. Chem. Soc.* **2005**, *127*, 7632-7637.
41. Guo, Y.-G.; Hu, J.-S.; Liang, H.-P.; Wan, L.-J.; Bai, C.-L. *Adv. Funct. Mater.* **2005**, *15*, 196-202.